Wall effect on fluid-structure interactions of a tethered bluff body

Sumant Sharma, Vrishank Raghav, Narayanan Komerath, Marilyn Smith

Daniel Guggenheim School of Aerospace Engineering
Georgia Institute of Technology, Atlanta, GA 30332-0150, USA

Abstract

Wind tunnel experiments have shown an unexplained amplification of the free motion of a tethered bluff body in the smaller wind tunnel relative to that in a larger wind tunnel. The influence of wall proximity on fluid-structure interaction is explored using a compound pendulum motion in the plane orthogonal to a steady freestream, with a doublet model for aerodynamic forces. Wall proximity amplifies a purely symmetric single degree of freedom oscillation with the addition of an out-of-phase force. The success of this simple level of simulation enables progress to develop metrics for unsteady wall interference in dynamic testing of tethered bluff bodies.

Keywords: Fluid-structure interaction, Bluff body, Wall effect, Instability, Sling load

Correspondence: vrishank@gatech.edu, Phone: 404-894-9622

1. Introduction

Fluid-structure interaction (FSI) arises due to the coupling between unsteady fluid flow and structural motion of the bluff body, in several engineering problems [1]. For instance, bluff body loads suspended from a helicopter at a single point, allow for several degrees of freedom of motion [2]. The possibility of large oscillations due to FSI limits the domain of safe operation. Such FSI problems involve a variety of dynamic phenomena over a wide range of flow parameters. Williamson [3] shows that prior work in this area has focused mainly on vortex-induced vibrations.

Tethered bluff body studies are often conducted using scale-model experiments [4, 5] in wind or water tunnels. In aerodynamic literature, blockage is a term used to describe the ratio of the projected area occupied by the body to the total test section area of the wind/water tunnel. Blockage is a constraint which is experienced by a body immersed in a moving fluid bounded by rigid walls. The walls prevent the free displacement of the airflow by the body resulting in unrealistic pressure distributions. A comprehensive review of subsonic wall effects is presented by Garner et al. [6]. Wall interference effects on unsteady experiments have been studied primarily for oscillating wings and are presented in [6, 7]. The acceptable level of blockage posed by the body in the tunnel is a significant parameter in selecting the maximum model scale (and is generally set at 5 percent of the cross-sectional area of the tunnel test section). The issue that

Email addresses: vrishank@gatech.edu (Vrishank Raghav), komerath@gatech.edu (Narayanan Komerath)

motivated this study is the possibility that unsteady motion causes unexpected wall effects that contaminate measurements, even when the static blockage is within accepted limits.

A high-fidelity prediction of such interactions would require a well-resolved time-dependent fluid dynamic computation combined with a 6-degree-of-freedom dynamics model and structural dynamics of the tether and body system. This would require large computational resources. This letter reports exploratory results on a rapid potential flow technique to identify how a proximal wall would affect unsteady bluff body FSI. Such a technique can provide physical insight and the ability to experiment with many combinations to represent various interaction mechanisms. A fundamental simulation of instability mechanisms would also enable confident prediction of the performance of such loads at different speeds and sizes. This simulation technique could become a powerful tool to gain and use physical insight of dynamic-aerodynamic response of tethered bodies using a consistent mathematical framework.

2. Motivation and hypothesis

The motivation was derived from observing results from wind tunnel experiments conducted on a tethered rectangular bluff body in two wind tunnels (test section dimensions - $2.74m \times 2.13m$ and $1.07m \times 1.07m$). At low speeds, roll oscillations accompanied by yaw were seen to amplify only in the $1.07m \times 1.07m$ tunnel. The divergence speed (defined below) measured in the $1.07m \times 1.07m$ tunnel was thus substantially lower than that seen from tests in the $2.74m \times 2.13m$ tunnel.

Divergence was defined as a condition where the amplification rate is above a certain threshold, or the amplitude of oscillations exceeds a specified threshold, either case triggering concerns about vehicle safety. Good guidance on the mechanisms that are in play would enable alleviation techniques or quantitative metrics to guide safety decisions. Several basic mechanisms can be considered for the initiation of divergence. In each of these listed below (illustrated in Table 1), different phenomena must interact to amplify the motion.

1. Yaw oscillations induced by:
   (a) Lateral motions (rolling) of the body
   (b) Unsteady flow experienced by the body
   (c) Phenomena which causes an asymmetric C_p
2. Yaw oscillations can also couple with pitch through the action of drag forces that create fore-aft swing.
3. Yaw and lateral swing induced by vortex shedding.
4. Vortex shedding drives periodic drag oscillations, coupling angle of attack with yaw.

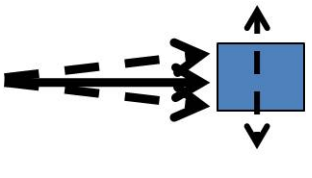	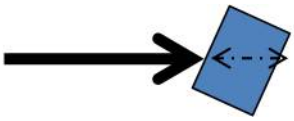
Yaw Oscillations	Yaw coupled with Drag
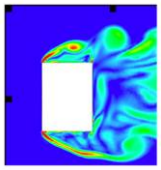	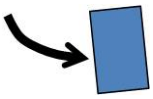
Yaw due to vortex shredding	Yaw due to helicopter maneuvers

Table 1: Basic mechanisms for amplification

3. Methodology

A sequence was developed to computationally simulate the different degrees of freedom in the motion of the tethered box. Degrees of freedom were added one at a time. The body was modeled as a rigid body on a compound pendulum as illustrated in Figure 1(a). The model accounts only for one single sling that is attached to the center of the top surface of the box unlike the wind tunnel experiments where the box had four slings. Conservation of angular momentum for a rigid body in two dimensional motion gives:

$$I_{xx}\ddot{\alpha}_P = \sum M_P - \mathbf{r_{pc}} \times m_T \mathbf{a_p} \tag{1}$$

where, I_{xx} is the mass moment of inertia of the bluff body along x-x axis about point P, M_P is the moment balance about point P, r_{pc} is the displacement vector of P from center of mass C, m_T is the total mass of the body and a_P is the acceleration vector of the point P.

Since the pivot point P is stationary, equation 1 simplifies to:

$$I_{xx}\ddot{\alpha}_P = \sum M_P \tag{2}$$

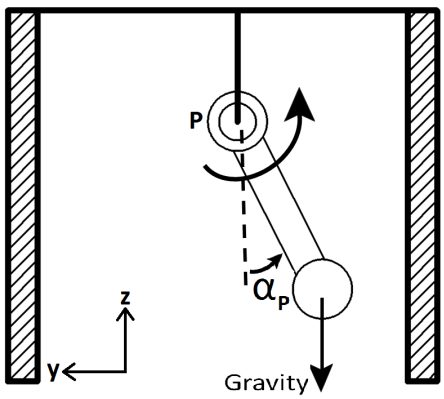

(a) Pendulum model

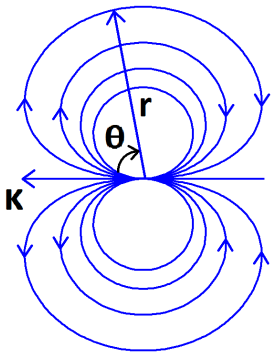

(b) A discrete 2D doublet with strength κ

Figure 1: Details of the pendulum model and doublet element

$$I_{xx}\ddot{\alpha}_P = -mgl\sin(\alpha_P) \tag{3}$$

where g is the acceleration due to gravity, l is the length of the tether, and α_P is the angular displacement.

The bluff body was modeled using a 2D doublet placed at the center of the bluff body. The walls were modeled using the method of images, essentially using the images of the doublet to model the effect of the wall. The interaction of a freestream and a doublet provides two components of velocity. The components are separated into radial and orthogonal directions. Using the velocity potential due to a doublet, the velocity at a point is given by:

$$V_R = \left(U_\infty - \frac{\kappa}{r^2} \right) \cos(\theta) \tag{4}$$

$$V_\theta = \left(-U_\infty - \frac{\kappa}{r^2} \right) \sin(\theta) \tag{5}$$

where V_R and V_θ are the radial and orthogonal components of induced flow velocity by the doublet (see figure 1(b)), U_∞ is the freestream velocity, κ the doublet strength, and r is the distance from the doublet

Once the velocity was determined, the pressure was determined using the Bernoulli equation for incompressible flow, assuming isentropic flow and thus constant stagnation pressure. This determines the force due to the induced velocity at each point and thereby the forcing function due to the wall. It should be noted that the velocity of the swinging pendulum motion is very small compared to the freestream velocity. In this model, there are six different velocities that must be accounted for the sides of the bluff body that face the walls. After calculating the dynamic pressure ($q = \frac{1}{2}\rho V^2$) due to each of the velocities, a force for

Step	Elements used	Walls	Remarks
1	Pendulum + Doublet + Freestream	✗	No amplification
2	Pendulum + Doublet + Freestream	✓	No amplification
3	Case 1 + Out of phase force	✗	Amplification
4	Case 1 + Out of phase force	✓	Higher rate of amplification

Table 2: Simulation conditions

each face (facing the wall) was calculated. This force was expressed in a form of linear momentum and then added to the differential equation governing the motion of the pendulum. Equation 3 now becomes:

$$I_{xx}\ddot{\alpha}_P = l \cdot F - mgl\sin(\alpha_P) \tag{6}$$

The sign of F determined whether the force would be added or subtracted from the harmonic motion due to mass of the box. The mathematical formulation and simulation were done using MATLAB® and Simulink®. The steps are given below and summarized in Table 2.

1. The first case simulates the harmonic motion of a pendulum $\left(\frac{\mathrm{d}^2\alpha_P}{\mathrm{d}t^2} + \frac{g}{l}\sin\alpha_P = 0\right)$ in the presence of a doublet and a freestream. The doublet is placed at the present location of the bluff body and acts as a circular body in the flow when a freestream is added. Mass and tether length of the tethered body are the same as those in the wind tunnel experiments to maintain consistency for eventual experimental verification. The body is subject to an initial condition of $\alpha_P = 30°$ where α_P is the angle measured from the sling axis when the pendulum is at rest.

2. In this case, two imaginary doublets were added behind the physical location of the walls to mirror the doublet on the pendulum. Their location changes with the location of the center doublet and was determined at each step of the simulation to satisfy the wall boundary conditions. As the pendulum gets closer to one wall of the test section, doublets changed their locations accordingly to maintain boundary conditions and simulate the effect of a physical wall.

3. In the third step of the demonstration yaw oscillations were simulated in the absence of a force due to the mirrored doublets. This accounts for the case where the box was allowed to roll freely due to the harmonic pendulum motion and was subject to a yawing oscillation. The effect of yaw was simulated as a force which is at the same frequency but out of phase with the pendulum motion. A Fourier Transform analysis of the pendulum motion from the first step gave a frequency of 3.767 rad/s. This frequency was introduced in the Simulink® model using of a sine wave given by:

$$F(t) = 0.056\sin\left(\ 2\pi\ (0.5998) + \frac{\pi}{2}\right) \tag{7}$$

4. In the fourth step of this demonstration, two degrees of freedom for the pendulum were introduced by adding the moment due to the force exerted by the mirrored doublets as well as an out of phase forcing function to simulate the yaw oscillations. For convenience, the derivative block shifts the phase by 90 degrees with respect to the pendulum motion, to model the effect of yaw.

4. Results and Discussions

The first natural frequency of the tethered bluff body system used in the wind tunnel was measured in free quiescent air to be 3.737 rad/s. This agreed to within 0.8% with the value of 3.767 rad/s obtained from simulation. For Case 1, the expected harmonic motion from -30° to +30° was obtained. Case 2 simulation results in a constant wall force amplitude, equal in magnitude and opposite in direction periodically and hence not contributing any resultant forcing to the periodic motion. This fact is reaffirmed by the results from the Simulink® model simulation of the pendulum motion.

The amplitude of the out of phase force relative to that of the primary wall effect force (Case 3) was selected to be 0.056 in order to make the instability evident within the simulation time. The appropriate range of amplitudes from aerodynamic loads must await further investigation through correlation with quasi-steady load data and dynamic measurements from the wind tunnel and computational fluid dynamics. Case 4 again shows the pendulum oscillation amplifying (See Figure 2) due to wall proximity.

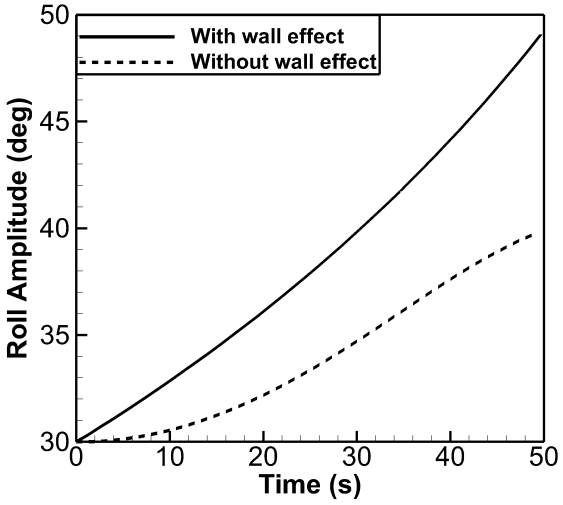

Figure 2: Amplification of the pendulum motion when coupled with an out-of-phase force

5. Concluding remarks

In this letter, a sequence of simple mathematical simulations is used to illustrate how to simulate the basic mechanisms by which a tethered bluff body may develop divergent oscillations in the presence of a proximal wall. In summary,

1. The flow between the box and the tunnel walls produces a suction which in turn produces a force on the box. With one degree of freedom this suction is symmetric and does not contribute to instability.

2. With two degrees of freedom, namely a lateral swing and a forcing function that is out of phase with the lateral swing, divergence occurs in the motion of the box.

3. Amplification rate is seen to depend on the proximity of the walls.

This simulation can thus provide guidance on the effects of proximal walls in amplifying the oscillations due to FSI of a tethered bluff body. Although motivated by the case of unsteady wall effect, a potential flow simulation framework at this level of complexity shows promise to provide physical insight into tethered bluff body instability mechanisms, and the role of interaction between degrees of freedom. Complex pressure distributions and tether dynamics could be systematically introduced into the simulation to study instability mechanisms.

6. Acknowledgment

This work is funded through the U.S. Army/NASA Vertical Lift Rotorcraft Center of Excellence at Georgia Institute of Technology.

References

[1] E. Naudascher, D. Rockwell, Flow-induced vibrations: an engineering guide, volume 7, Dover Publications, 2005.

[2] Multiservice Helicopter Sling Load: Single-Point Load Rigging Procedures, CreateSpace Independent Publishing Platform, 2003.

[3] C. Williamson, R. Govardhan, Annu. Rev. Fluid Mech. 36 (2004) 413–455.

[4] C. Williamson, R. Govardhan, Journal of fluids and structures 11 (1997) 293–305.

[5] K. Ryan, C. Pregnalato, M. Thompson, K. Hourigan, Journal of fluids and structures 19 (2004) 1085–1102.

[6] H. Garner, E. Rogers, W. Acum, E. Maskell, Subsonic wind tunnel wall corrections, Technical Report, AGARD, 1966.

[7] R. Vos, Technical Report, NATO Science and Technology Organization, 1998.